Present status of negative ion based NBI system for long pulse operation on JT-60U

Y. IKEDA, N. UMED, N. AKINO, N. EBISAWA, L.GRISHAM*, M. HANADA, A. HONDA, T. INOUE, M. KAWAI, M. KAZAWA, K. KIKUCHI, M. KOMATA, K. MOGAKI, K. NOTO, F. OKANO, T. OHGA, K. OSHIMA, T. TAKENOUCHI, Y. TANAI, K. USUI, H. YAMAZAKI, T. YAMAMOTO

Japan Atomic Energy Research Institute, 801-1 Mukouyama, Naka, Ibaraki-ken, 311-0193, Japan
**) Princeton Plasma Physics Laboratory, Princeton, New Jersey, USA*

The 500-keV negative-ion based neutral beam injector for JT-60U started operation in 1996. The availability of the N-NBI system has been improved gradually through modifying ion source and optimizing its operation parameters. Recently, the extension of the pulse duration up to 30 sec has been intended to study quasi-steady state plasma on JT-60U. The most serious issue is to reduce the heat load on the grids for long pulse operation. Two modifications have been proposed to reduce the heat load. One is to suppress the beam spread which may caused by beamlet-beamlet interaction in the multi-aperture grid due to the space charge force. Indeed, the investigation of the beam deflection, which was measured by the infrared camera on the target plate set 3.5 m away from the grid, indicates the beam spread is in proportion to the current density. Thin plates were attached on the extraction grid to modify the local electric field. The plate thickness was optimized to steer the beamlet deflection. The other is to reduce the stripping loss, where the electron of the negative ion beam is stripped and accelerated in the ion source and then collides with the grids. The ion source was modified to reduce the pressure in the accelerator column to suppress the beam-ion stripping loss. Up to now, long pulse injection of 17 sec for 1.6 MW and 25 sec for ~1 MW has been obtained by one ion source with these modifications.

1. Introduction

A high energy beam at more than several hundred keV is required to heat high density plasma and to drive plasma current efficiently on magnetic fusion devices. The negative ion based neutral beam injection (N-NBI) system has been developed and constructed on JT-60U to inject high energy beam up to 500 keV. Through the successive operation from 1996, the injection power into plasma has gradually increased. In 2000-2001, the negative-ion current per ion source reached 20 A at 366keV for H^- and 17.4 A at 403 keV for D^-, and the maximum deuterium neutral injection power was 5.8 MW at 400 keV for 0.9 sec with two ion sources [1]. In 2002, the distorted electric field in the first acceleration gap, which was caused by a groove in the extractor grid, was corrected. This resulted in a reduction of the heat load on the NBI port limiter, and then the 10 sec operation was

achieved at the power level of 2.6 MW, 355 keV for H^- with one ion source [2]. In 2004, the extension of the pulse duration up to 30 sec has been intended to study quasi-steady-state plasma on JT-60U, where the NBI pulse duration is significantly longer than the plasma current diffusion time. The most serious issue is to reduce the heat load on the grid because the temperature of the cooling water at the acceleration grid reached up to ~100°C for the pulse duration of 10 sec at the injection power of 2.6 MW.

In this report, the improvements of the heat load on the grid are proposed. One is to locally adjust the beam deflection to avoid the beam direct interception in the ion source. The other is to reduce the striping loss, where the electron of the negative ion beam is stripped and accelerated in the ion source and then collides with the grids.

2. Status of JT-60U NBI system

In JT-60U, high performance plasmas have been developed to provide a physics basis for ITER [3] and advanced steady-state tokamak reactors such as SSTR [4]. To realize a steady-state operation in a fusion reactor, it is important to study long pulse plasmas with high performance where the time scale is longer than the current diffusion time and close to the wall saturation time in ELMy H-mode. The pulse duration of JT-60U has been extended from 15 sec to 65 sec to address the new research towards the prolongation of plasma performance [5]. The pulse duration of NBI has been also required to extend from 10 sec to 30 sec. In the positive ion based NBI, four tangential injection units have successfully extended their pulse duration up to 30 sec at the power level of 2MW each by the modification of the power supply, beam limiters, and control systems. Though the pulse duration of other seven perpendicular injection units is unchanged (10 sec), their control systems have been adjusted to perform the continuous 30 sec-operation in series. The injected energy reached 330 MJ with the positive ion based NBI in 2004 [6].

In the negative ion based NBI, there are two (lower and upper) ion sources mounted on a single beamline. The acceleration power supply, whose original capability is 500 kV, 64 A for 10 sec, has a cascade connection of three-stage potential and supplies the power to both the ion sourses in common. To extend the pulse duration from 10

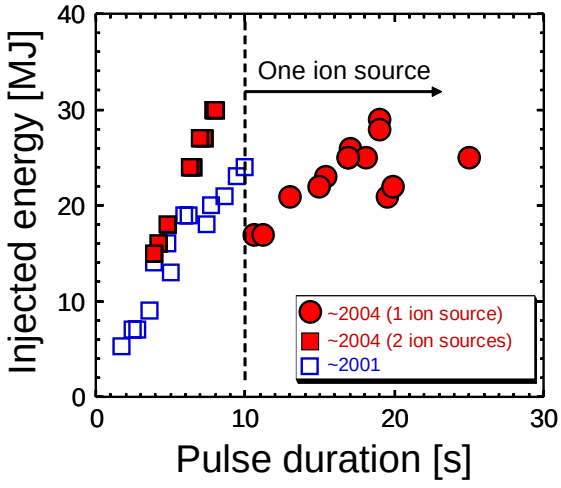

Figure 1. Progress of the injected energy in the long pulse operation.

sec to 30 sec, the lower ion source was modified and used to demonstrate its capability for long pulse operation within the capability of the power supply system. Figure 1 shows the injection beam energy as a function of the pulse duration before and after the modification. The maximum injected energy has reached up to ~30 MJ with the lower ion source in 2004. The pulse duration has been extended up to 25 sec at the power level of ~1 MW, where the optimization of the operational parameters has not been done due to the shortage of tuning and conditioning time in the last campaign. Though the injection power is still low, it was noticed that the temperature of the cooling water for the grill saturated at less than 70°C at 1.6MW with 20 sec operation. This result shows its capability for further long operation in next campaign.

3. Grid structure and measurement of beam deflection

The JT-60U N-NBI has two negative ion sources, each of which has five segments to extract and accelerate the negative ion beams. The ion extraction area in the ion source is 450 x 1100 mm to extract the negative ion current up to 22 A. Each segment, whose dimension is 450 x 180 mm, is composed of the plasma grid (PLG), the extractor grid (EXG) and three accelerator grids (A1G, A2G and GRG). Each grid has a 24 (horizontal) x 9 (vertical) aperture array to inject multiple beamlets into plasmas. The PLG carries a longitudinal current to induce a uniform transverse magnetic field that is required to enhance the negative ion yield [7]. The apertures with a diameter of 16 mm are arranged with the pitch of 19 mm, 21 mm in the horizontal and vertical directions, respectively. Dipole magnets are installed in the EXG. An aperture displacement of 0.5 mm is employed at the outlet of EXG to compensate the beam deflection due to the dipole magnetic field. On the final acceleration grid (GRG), the other aperture displacements in the horizontal and vertical directions are used to focus the beamlet

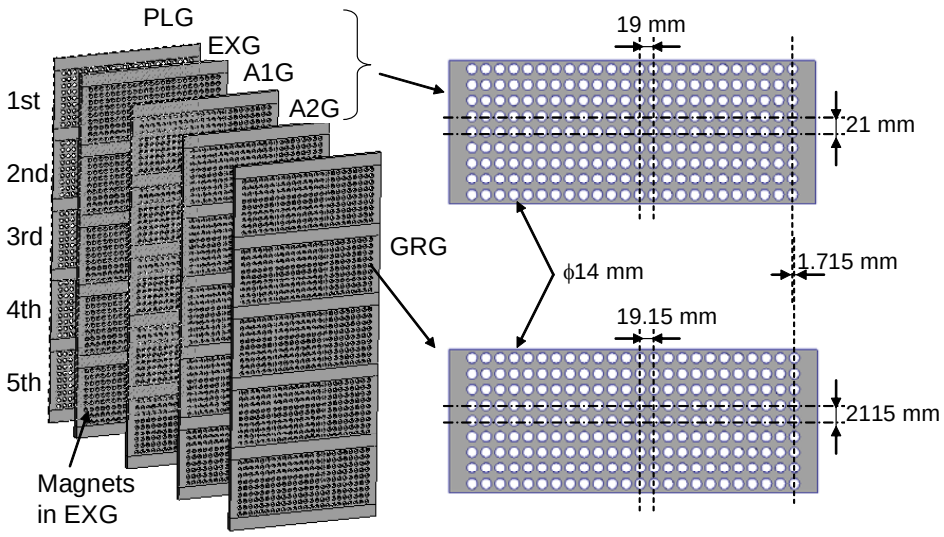

Figure 2. Grid structure of the JT-60U N-NBI system. There are five segments to generate negative ion current up to 22 A, each of which is composed of PLG, EXG, A1G, A2G and GRG. Dipole magnets are installed in the EXG. The aperture pitches of PLG-A2G and GRG are 19 mm and 19.15 mm in the horizontal direction, 21 mm and 21.15 mm in the vertical direction, respectively.

bundle from the large segment to the narrow NBI port, where the displacement increases with the distance from the center of the segment. The maximum displacement in the horizontal direction is 1.725 mm at the edge aperture. The heat load on each GRG segment was measured by calorimetry of the cooling water. Figure 2 shows the grid structure of the N-NBI ion source.

The beam deflections are directly measured by the temperature profile footprint at the target plate set at 3.5 m away from the ground grid of the upper ion source. An infrared camera, whose time frame is 120/s with a space resolution of ~3mm on the target plate, measures the beam profile footprint as shown in Fig.3. The target plate, which is a Molybdenum flat plate of 12 mm thickness without cooling, is removable to measure the beam profile between the injection shots. Some thermocouples are installed on the plate to calibrate the infrared measurement. Figure 4 shows the typical infrared view on the target plate of the upper ion source, where the profile is evaluated by subtracting the second flame from the initial flame at the time response of 8.3 ms. Five segments are clearly observed, each of which is composed of the multiple beamlets.

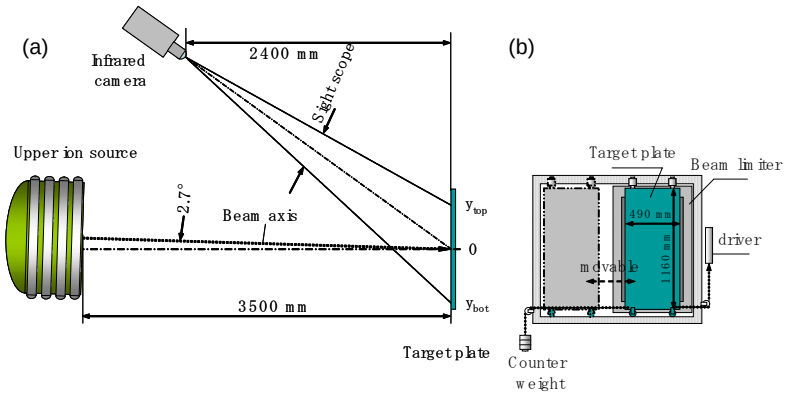

Figure 3. Measurement system for the beam deflection by an infrared camera. (a) Infrared camera system, (b) movable target plate.

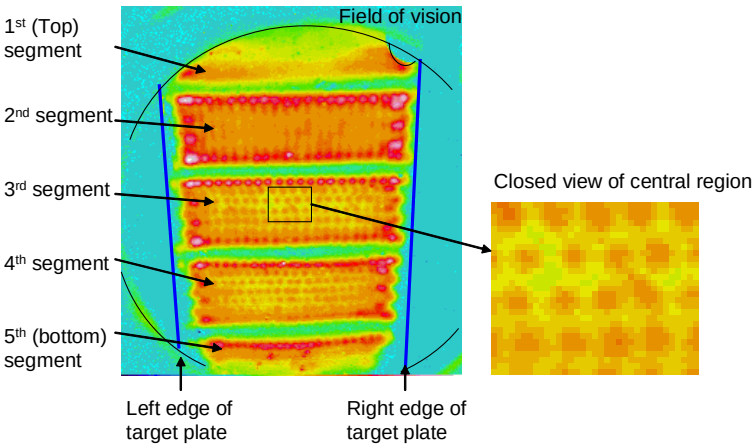

Figure 4. Typical infrared view on the target plate of the upper ion source.

3. Reduction of the heat load on the grid for long pulse operation

There may be two principal reasons for extra heat load on the grids. One is the direct interception of the negative ion beam on the grids. The grids were designed to pass and accelerate the negative ion through the grid apertures. It is required to steer the multi-beamlets so as not to cause beam bombardment on the multi-aperture grid. The other is the stripping loss, which may cause the electron bombardment on the grids, as well as impact by some of the fast neutrals arising from stripping. On both ion sources, the local electric field of the grid was modified to improve the beam

deflection for long pulse operation. The effect of the modification of the local electric field was investigated with the upper ion source by the infrared camera. Moreover, the lower ion source was modified to reduce the stripping loss by improving the vacuum conductance, which was expected to keep low pressure at the acceleration column

3.1 Beam Steering in multi-aperture grid

The trajectory of the beamlet is determined by the grid structure and the operational parameters such as the beam perveance, the dipole magnetic field for electron suppression, and aperture displacement for beam steering as shown in Fig.5. The negative ion beam is deflected by the dipole magnetic field at the EXG, and its deflection is compensated by the aperture displacement of the outlet of the EXG. The aperture displacement at the GRG is to steer and focus the multi-beamlets to the JT-60U plasma ~22m away from the ion source. In the original design of the ion source, the grid structures were determined based on test module results at the beam energy of 400keV with a small number of apertures in a grid, and with all the aperture offsets within a row in the same direction, so there was no space-charge compression [8]. However, it seems to be difficult to compensate the deflection angle for all operational parameters, because the magnetic deflection depends on the inverse of the Larmor radius of the ion beam, which is a function of the extraction (V_{ext}) and acceleration voltages (V_{acc}). Moreover, a beamlet-beamlet interaction in the multi-aperture grid due to the space charge force may become significant for high current operation [9]. Therefore, it is very important to experimentally investigate the beam deflection of the ion source, which has a 24x 9 aperture array in the segment.

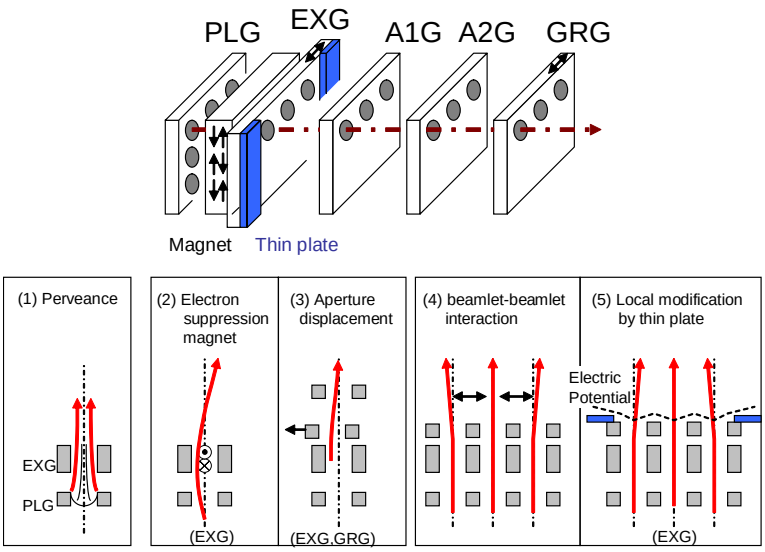

Figure 5. Keys for steering the beam deflection in the ion source.

First, the effect of the dipole magnetic field was studied. The dipole magnetic field is to separate the electron and negative ion beams due to their Larmor radius. The electron beam is deflected and collides with the EXG, while the negative ion beam is slightly deflected and passes through the aperture of the grids. The aperture displacement of the outlet of the EXG was designed to compensate this deflection. In the infrared view of the target plate, the multi-beamlets footprint in

the segment are featured by the lag between each line (Fig.4). This deflection is attributed to the dipole magnetic field in the EXG as reported in ref [10]. Figure 6 shows the displaced distance of the beamlets row in the horizontal direction on the footprint as a function of the extraction voltage at the condition of V_{ext}/V_{acc} ~0.017. The data in this figure is obtained at the central beamlets of the segment. where beamlet-beamlet interaction may be small due to cancellation of the space charge force between each other. It is found that the displaced distance decreases with the extraction voltage and that the distance is less than ~5 mm at V_{ext}/V_{acc} =6kV/ 360 kV. This result indicates that the deflection of the dipole magnetic field is well compensated in the operational region.

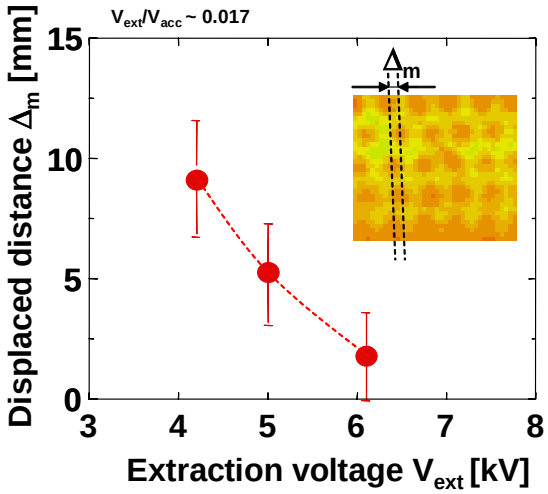

Figure 6. Displaced distance of beamlets row in the horizontal direction as a function of the extraction voltage. The rate of Vext/Vacc is set at ~0.017.

Second, the spread of the beamlet-bandle was investigated. In the multi-aperture grid, the beam deflection may be strongly enhanced at the edge beamlets in each segment, where space charge force is not canceled from the adjacent beamlets. This results in the expansion of the beamlet-bandle. To reduce the expansion, a thin plate was attached on the EXG to adjust the local electric field as shown in Fig.7.

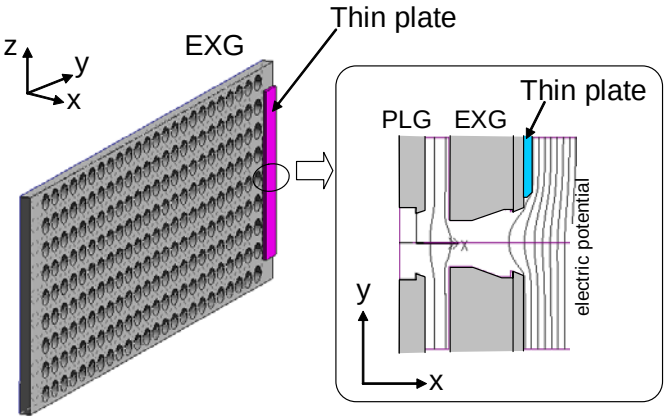

Figure 7. Attachment of thin plate near the seven apertures at edge column. The thin plate modifies the local electric field to steer the beamlet inwards.

The measured infrared view is shown in Fig. 8, where the thin plate is attached on left side to modify the local electric field of seven apertures. It is found that the width of the segment of left side is shorter than that of the right side without thin plate. The Figure 9 shows the displacement of the footprint from the geometrical pitch of the apertures as a function of plate thickness, where the middle (3rd) segment is only used to accurately estimate the averaged current density

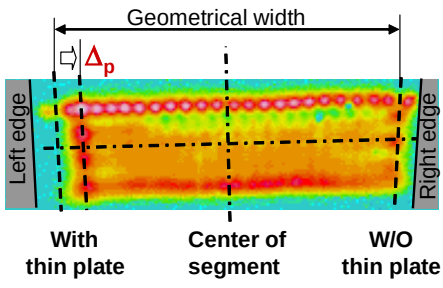

Figure 8. Typical infrared view of the middle segment with and without thin plate at edge. The edge beamlets except top and bottom row are modified by the attachment of the thin plate.

of this segment. The extraction, acceleration voltages, and averaged current density are V_{acc} =370-380 kV, V_{ext} =5.7~6.8 kV and j_{acc} = ~16 mA/cm^2, respectively in this operation. The expected design value in the horizontal direction is ~ - 10 mm to focus the beam bundle. Then thin plates of 2 mm and 1.5 mm thickness has been employed on the edge of the segments in the horizontal and vertical directions in order to steer the beamlets inwards against the beamlet-beamlet interaction. After the modification of this plate attachment on both sides, the heat load was measured at the condition of V_{ext}/V_{acc} ~6.5 kV/350~360 kV. Though the heat load of the GRG may depend on the beam perveance, it is shown that the heat load of the GRG is improved by the thin plates at the same operational condition as shown in Fig.10.

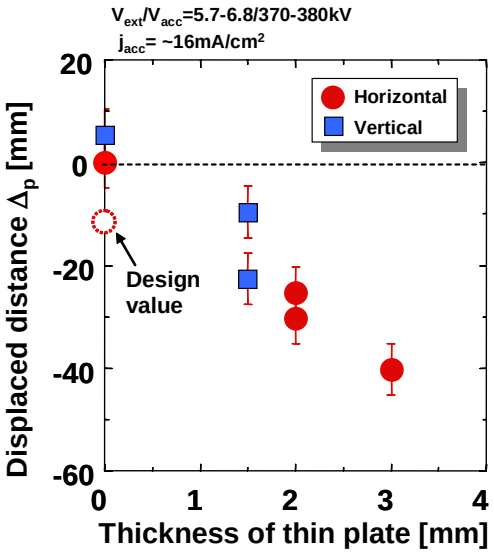

Figure 9. Displaced distance from the geometrical pitch of the aperture as a function of the thickness of the thin plate. Design value is evaluated by the aperture displacement of the GRG in the horizontal direction.

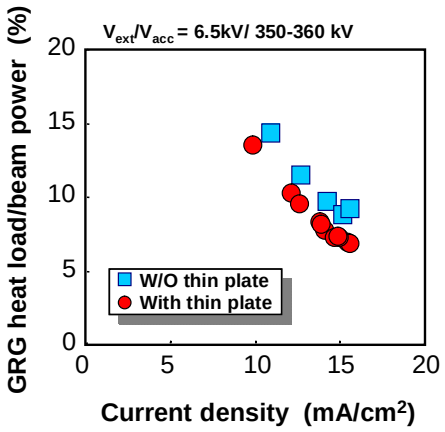

Figure 10. The heat load of the GRG normalized by the beam power as a function of the current density with and without the thin plate. The rate of Vext/Vacc is 6.5 kV/ 350~360 kV for both operation.

Then, the effect of the current density on the spread of the beam bundle was studied in the case of the 2mm-thickness plate. The infrared view of the target plate indicates that the temperature of each segment area is not the same, probably due to the non-uniformity of the source plasma [11] as shown in Fig. 11. The upper three and lower five rows of apertures in the top and bottom segments, respectively, are masked because the ion current is too small to maintain matched perveance in the extractor and accelerator. It is found that width of footprint of each segment depends on the current density of the segment as shown in Fig.12, where the current density of the each segment is estimated by assuming the current density is proportional to the averaged temperature of each segment. Since the thickness of the thin plate is adjusted for the middle segment at the current density of ~16 mA/cm^2, the beam steering may be too large for the top and bottom segments at low current density. The heat load of the top and bottom segments normalized by the extracted aperture

number is 0.75~0.8 kW in this parameter region, which is slightly larger than the middle segment (~0.7 kW). The head load at top and bottom segments may be enhanced by the over-deflection due to the thin plate, in addition to the non-optimized perveance at the low current density. In the future the thickness of the thin plates needs to be adjusted to be proportional to the current density for each segment.

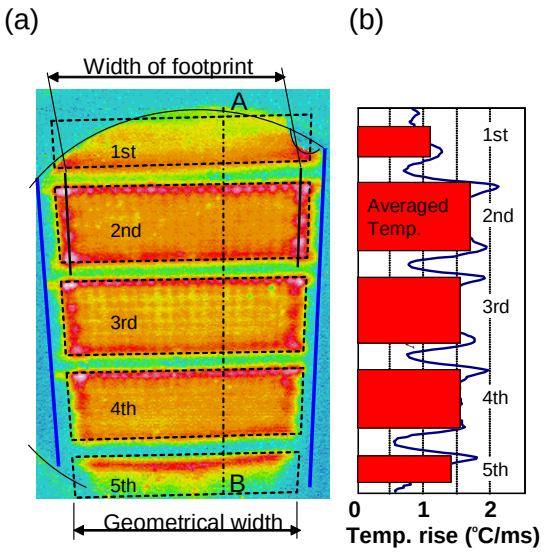

Figure 11. Width of the footprint at the target plate. (a) Typical infrared view for analysing the width of the beam bundle. Dotted lines show the geometrical width of the segment. (b) Temperature profile in the vertical direction (A-B in Fig.11(a)). The averaged current density is given by the averaged temperature in each segment.

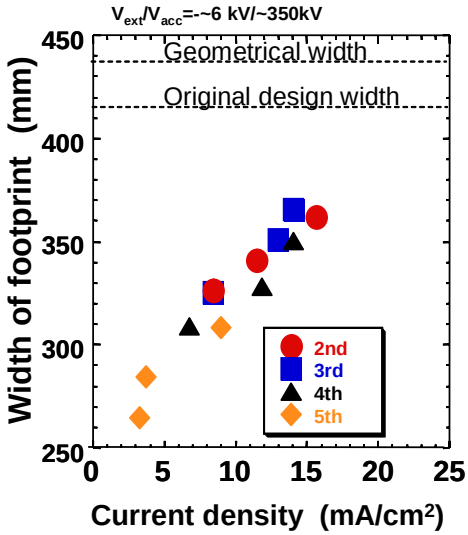

Figure 12. Width of footprint as a function of the current density in each segment. The rate of Vext/Vacc is ~6 kV/ ~350 kV in this data. Original design value is given by the aperture displacement of the GRG on the assumption of no bemalet-beamlet interaction.

3.2 Stripping loss

To reduce the stripping loss, the acceleration grids of the top and bottom segments of the lower ion source were vented to increase the vacuum conductance in the accelerator column. The PLG of these segments were entirely masked so as not to extract negative ion beams. This modification was expected to lower the pressure in the acceleration column. The thin plates were attached around the segments to compress the beamlet bundle. Figure 13 shows the pressure dependence of the heat load on the GRG at the acceleration voltage of 350 kV, extraction voltage of 6.4 kV and current density of ~14

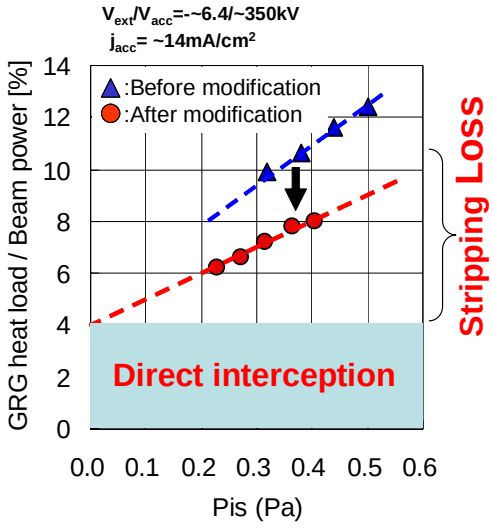

Figure 13. The heat load of the GRG before and after modification of vacuum conductance in the accelerator column.

mA/cm^2, respectively, where the heat load is normalized by the beam power and the pressure is measured in the ion source. The data before modification was measured with the original grids without thin plates. The heat load of the GRG normalized by the beam power is reduced from ~10 % to ~7 % after the modification [12]. It is apparent that the heat load increased linearly with the pressure, but the slope the pressure dependence of the heat load became weaker after the modification. The offset of the heat load at zero pressure in this figure may be mainly due to the direct beam interception, which has little pressure dependence. The modification of the ion source shows that lower pressure in the acceleration column is effective in reducing the heat load on the grids. The total injected power is only slightly reduced even though two of five segments are masked due to the non-uniformity of the negative ion generation. To increase the injected power for long pulse operation, a new approach to increase the vacuum conductance without masking the top and bottom segments will be developed when better uniformity of the negative ion generation is established in the future.

4. Discussion

The single beamlet trajectory was calculated by using EelcNet & MagNet 3-D code [13], which can take the dipole magnetic field, thin plates, and aperture displacement into account. Though the space charge effects on the perveance and beamlet-beamlet interaction are not treated in this calculation, the three dimensional beam deflection due to the grid structure can be estimated. The initial starting point of a D^- ion is given at the center of the PLG. Figure 14 shows the simulation model for the single beamlet calculation. The magnetic field produced by PLG current is omitted in this model, because the PLG magnetic field deflects the ion beamlet only a little in the vertical direction alone. The dipole magnets were inserted in the EXG between apertures. The center of the outlet aperture of the EXG is shifted by 0.5 mm. In the first step, the single beam trajectory at the central beamlet of the segment is simulated, where the aperture displacement at GRG is not done, and the effect of the space charge force may be negligible in practice. Figure 15 shows the beam trajectory in the horizontal plane as a function of the extraction voltage, where the V_{ext}/V_{acc}=0.017. In the case of aperture displacement of 0.5 mm at the EXG, the

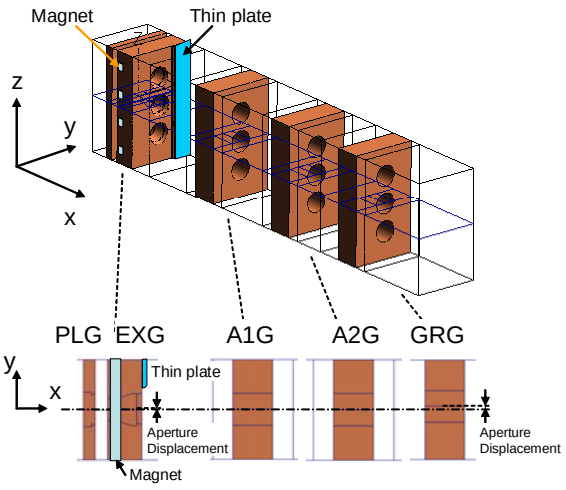

Figure 14. Simulation model for the single beam trajectory in the ion source. Dipole magnetic field in the EXG, aperture displacements of the outlet of the EXG and GRG, and thin plate at the EXG are taken into account.

dislpacement distances at 3.5 m away are 2.7 mm, 1.6 mm, 0 mm and 1.5 mm for V_{ext}/ V_{acc} = 4.2 kV/ 250 kV, 5 kV/ 300 kV, 6 kV/ 350 kV and 8.2 kV/ 500 kV, respectively, calculated from the simulation results. It is shown that the aperture displacement of the outlet of the EXG well compensates the deflection due to the dipole magnetic field and that the calculated beam deflection is of the same level as the measured one as shown in Fig.6.

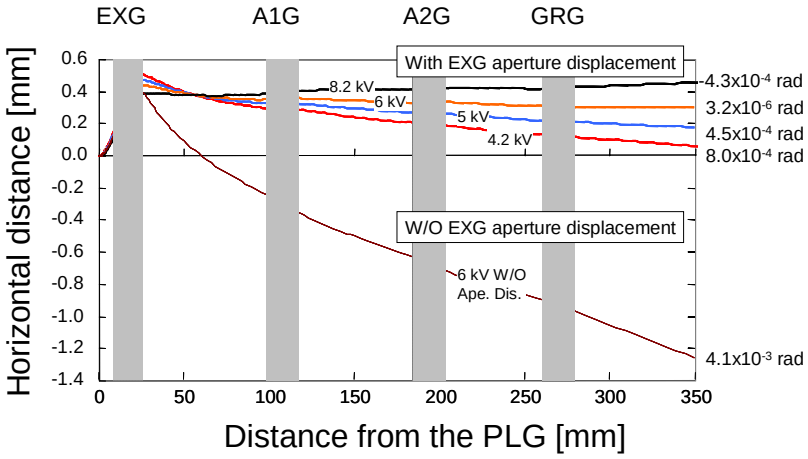

Figure 15. Effect of the beam trajectory on the aperture displacement of the outlet of the EXG when the extraction voltage are changed from 4.2 kV to 8.2 kV at Vext/Vacc of ~0.017.

In the second sta ge, the effect on the edge beamlet of the thin plate is calculated. The aperture displacement of the GRG at the edge beamlet is 1.725 mm in the horizontal direction. The original design was to steer the edge beamlet inward by this aperture displacement alone. Figure 16 shows the single beamlet trajectory as a function of the thickness of the thin plate. Without the thin plate, the beam deflection angle θ_d is about 2.6×10^{-3} rad due to the aperture displacement at the GRG, which satisfies the design specification and agrees with the electrostatic lens formula of $\theta_d = E_{grid}/(4V_{beam})\delta$ (where E_{grid}: electric field between A2G and GRG, V_{beam}: beam energy, δ: aperture displacement). It is also shown that the modification of the local electric field at the EXG is effective to deflect the negative ion beamlet and that the displaced distance of the beamlet is almost in proportion to the thickness of the thin plate. On the contrary, the infrared measurement of the beam deflection at the target footprint is 25~30 mm, which corresponds to a deflection angle of $7\sim8.5\times10^{-3}$ rad. Moreover, the experimental beam trace on the GRG, which was directly measured during the inspection of the ion source after operation, shows that the beam trace at the inlet of the GRG is shifted ~ 1mm inwards from the geometrical aperture pitch axis. These measured deflections, which resulted from operation with a 2 mm-thickness plate, agrees with the simulation results in the

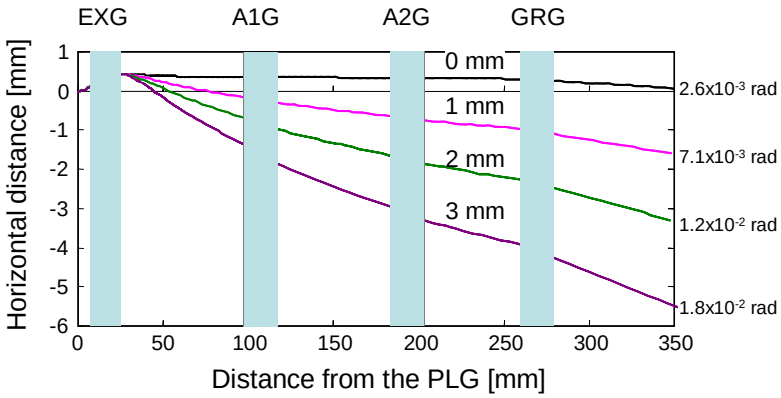

Figure 16. Effect of the beam trajectory on the thin plate when the thickness is changed from 0 mm to 3 mm at Vext/Vacc of 6 kV/ 350 kV.

case of a 1 mm-thickness plate. This result indicates that the space charge force between beamlets is significantly large and seems to disturb multi-beamlets from passing through the multi-aperture gr id, especially at the edge beamlets. Therefore, it is required to modified and optimize the grid structure by taking account of the beamlet-beamlet interaction, current density and vacuum conductance for further long pulse operation. A multi-slit grid [14] with the thin plate is one of the candidates to improve the vacuum conductance and flexibility against the beam misdeflection, which may change with operational parameters.

4. Summary

On the JT-60U N-NBI system, long pulse operation was carried out using the modified ion source with increasing vacuum pumping conductance and thin plates on the extraction grid. Up to now, the pulse duration has been extended up to 25 sec at ~1 MW and 17 sec at 1.6 MW. Temperature saturation of the cooling water for the accelerator suggests that further expansion of the pulse duration can be expected after sufficient conditioning of the ion source.

It is found that the local modification of the electric field by attaching a thin plate is useful to suppress the beam spread due to the space charge force, which may affect the heat load of the multi-aperture grids. Since the beam deflection depends upon the current density, the thickness of the field-shaping plates needs to be proportional to the current density in each grid segment, because of the non-uniformity of the negative ion production in these sources [1]. Further modification of grid structure, taking better account of space charge interaction, may be expected to further improve the performance of the multi-aperture grid.

Acknowledgments

The authors want to express our thanks to thank the members who have contributed to the JT-60U project especially for modification to the long pulse operation. They wish to express their gratitude to Drs. Kuriyama and Hosogane and to the Plasma Heating Laboratory in JAERI for useful discussion for the long pulse operation of N-NBI system on JT-60U.

References

[1] Kuriyama,Y., et al., Fusion Sci. Tech., **42** (2002) 410.

[2] Umeda, N., et al., Nucl. Fusion **43** (2003) 522.

[3] ITER Technical Basis, ITER EDA Documentation Series No.24, IAEA, Vienna, 2002.

[4] Nishio, S., at al., Fusion Energy 2000, Sorrento, Italy, 2000, FTP2/14, IAEA (2000).

[5] Ide, S., et al., Fusion Energy 2004, Vilamoura, Portugal, 2004,OV/1-1, IAEA (2004).

[6] Akino, N., et al., to be published to Fusion Sci. Tech., (Proc. 16th ANS Topical Meeting on the Tech, of Fusion Energy, Madison, USA, 2004).
[7] Okumura, Y., et al., Proc. IEEE 14th Symp. Fusion Engineering, Hyannis, Massachusetts, P.466 (1993).
[8] Inoue, T., et al., “Steering of high energy negative ion beam and design of beam focusing/ deflection compensation for JT-60U large negative ion source”, JAERI-Tech 2000-023, Japan Atomic Energy Research Institute, 2000.
[9] Fujiwara, Y., et al., Rev. Sci. Instrum. **71** (2000) 3059.
[10] Takayanagi, T., et al., Rev. Sci. Instrum. **73** (2002) 1061.
[11] Kuriyama, M, et al., Proc. 18th IEEE/NPSS Symp. Fusion Engineering, Albuquerque, USA, (1999) 133.
[12] Umeda, N, et al., to be published in Fusion Eng. And Design, (Proc. 23rd Symp. Fusion Tech. , Venice, Italy, 2004).
[13] EelcNet & MagNet-3D, Version 6, Infolytica Corp, Canada.
[14] Tsumori, K., et al., Rev. Sci. Instrum. **75** (2004) 1847.